



HAL
open science

An empirical approach to parameterizing photovoltaic plants for power forecasting and simulation

Yves-Marie Saint-Drenan, S. Bofinger, R. Fritz, S. Vogt, G.H. Good, J. Dobschinski

► **To cite this version:**

Yves-Marie Saint-Drenan, S. Bofinger, R. Fritz, S. Vogt, G.H. Good, et al.. An empirical approach to parameterizing photovoltaic plants for power forecasting and simulation. *Solar Energy*, 2015, 120, pp.479-493. 10.1016/j.solener.2015.07.024 . hal-02286805

HAL Id: hal-02286805

<https://hal.science/hal-02286805>

Submitted on 13 Sep 2019

HAL is a multi-disciplinary open access archive for the deposit and dissemination of scientific research documents, whether they are published or not. The documents may come from teaching and research institutions in France or abroad, or from public or private research centers.

L'archive ouverte pluridisciplinaire **HAL**, est destinée au dépôt et à la diffusion de documents scientifiques de niveau recherche, publiés ou non, émanant des établissements d'enseignement et de recherche français ou étrangers, des laboratoires publics ou privés.

An empirical approach to parameterizing photovoltaic plants for power forecasting and simulation

Yves-Marie Saint-Drenan^{a,*}, Stefan Bofinger^a, Rafael Fritz^a, Stephan Vogt^a, Garrett H. Good^a, Jan Dobschinski^a

^a*Fraunhofer Institute for Wind Energy and Energy System Technology (IWES), 34119 Kassel, Germany*

Preprint submitted to Solar Energy in October 2015

Abstract

The aim of this work is to develop an algorithm that can utilize historical PV power measurements to establish the parameters of a physical model for power production. The chosen approach consists in evaluating the parameters of a PV model that maximize the likelihood that simulations match with power measurements. The proposed method offers advantages beyond the standard approaches used for the simulation or prediction of PV power production, as it makes maximum use of the information typically available on a PV plant (plant description and measurement history). Furthermore, an interpretation and control of the algorithm output is made possible. The performance of the proposed approach has been evaluated and analysed using measurements from two PV plants. It is shown that the proposed approach may identify the orientation angles of a PV module to within an accuracy of less than 2° in optimal cases. Situations were also found with a difference between the estimated and actual angles of 5° , for which the estimated parameters lead to better simulation/forecast accuracy than the actual ones as they balance the systematic error of the chosen PV-model.

Keywords: Photovoltaic, Simulation, Forecast, Characterization

1. Introduction

It has become commonplace for photovoltaic forecast suppliers or academic groups to need to generate forecasts for PV plants for which little information aside from historical power measurements is available. The two common approaches in this case are the physically motivated approach and the statistical approach.

The physically motivated approach maximizes the use of the information available for the plant (Drews et al., 2006; Kidwelly, 2006). Optimally, PV plant information includes orientation angles of the PV modules along with the module and inverter specifications. In this case, a calculation of the PV power from meteorological data using available models from the literature is possible. Systematic differences between the

*Corresponding author

Email address: yves-marie.saint-drenan@iwes.fraunhofer.de (Yves-Marie Saint-Drenan)

9 simulated/forecasted and measured power can however be frequently observed. This error typically results
10 from differences between the information used and the actual characteristics of the PV plants (approximate
11 module orientation, deviation from manufacturer specifications, etc. . .). A manual correction of the plant
12 information used is always possible, but may be time-consuming. The physical approach applies to ideal
13 conditions, but it is unfortunately often the case that its implementation is impossible due to missing PV
14 plant information needed for the calculation of the power from meteorological data.

15 The alternate approach is the statistical one, for which PV plant information is not a necessary prereq-
16 uisite. In this approach, the best possible use is made of historical measurements. Artificial neural networks
17 have become a standard practice to this end, and numerous works can be found in the literature on such
18 methods (de Rocha Vaz, 2014; Dolara et al., 2015; Espinar et al., 2010). Though a statistical approach
19 avoids the problems faced by the physical approach, other issues are present themselves. A neural network
20 or any other statistical method learns dependencies between input and output data using a training dataset.
21 For this purpose, it is important to exclude data affected by measurement errors or plant outages from
22 the training dataset that would hinder the training phase of the statistical method used. Though obvious
23 measurement errors can be easily detected and excluded from the training dataset, other errors like downed
24 power lines or module shading may be more difficult to identify. The performance of the statistical approach
25 is thus strongly dependent on the quality of the training dataset, which is sometimes difficult to guarantee.
26 In the case of a deficient training set, it is not possible to check or fit the statistical coefficients to make
27 manual fixes as were possible with the physical approach. Lastly, no use of the available plant parameters
28 can be made with the statistical approach.

29 Both the physical and statistical approaches thus have advantages and drawbacks, and the optimal
30 approach may depend on the quality of the available dataset. Still, neither approach is ideal as both ignore
31 some part of the available information: historical measurements are not used in the physical approach and
32 plant parameters is overlooked in the statistical approach.

33 Time series of power measurements implicitly contain a wealth of information on a PV plant. A visual
34 inspection of this data may for example easily reveal whether the PV modules are oriented to the east or the
35 west. This shows that it may be possible to derive (or train) parameters of a physical model from historical
36 measurements. Such a hybrid approach would offer many advantages. First, the simulation model could
37 integrate physical models available from the literature. Then, information contained in historical measure-
38 ments would be fully exploited. Finally, it would be possible to control and modify trained parameters,
39 which would have a physical sense. Regarding the last point, information available on a PV plant (module
40 orientation, inverter or module specifications) could be explicitly used for the validation or modification of
41 the assessed parameters.

42 The goal of the work presented in this paper is to develop a hybrid approach, in which parameters of a
43 PV model are estimated from historical PV power measurements and meteorological data. The focus of this

44 paper is consequently put on the choice of the appropriate configuration parameters of a PV model (module
45 azimuth and tilt angle, power curve, etc...), rather than on minimizing the forecast/simulation error. A
46 minimization of the error by e.g. removing systematic errors from the meteorological input data and/or by
47 means of model output statistical methods may be conducted once the parameters of the considered plant
48 are known, but this step is not addressed here.

49 Characterizing a PV plant requires estimating the parameters of a PV plant model that lead to the best
50 match between measurements and simulation. A preliminary step is to choose a PV model, which is the
51 focus of section [section 2](#). The approach used for assessing the parameters is then described in [section 3](#).
52 In [section 4](#), parameters of two plants are evaluated with the proposed approach; and compared with the
53 known plant characteristics. Advantages and limitations of the parameter estimation algorithm introduced
54 in this paper are then finally discussed in conclusion.

55 **2. PV plant model selection**

56 The aim of the proposed approach is to derive parameters of a PV model from historical measurements,
57 facilitating the simulation/forecast of the power production of a PV plant from meteorological data with
58 the best accuracy. This goal has two objectives at odds with one another. On one hand, the best simulation
59 accuracy is obtained by using complex models requiring detailed information on the configuration of a PV
60 plant. Though power measurements implicitly contain a lot of information on a PV plant, it is clear that
61 it is not possible to ascertain each detailed characteristics of a PV plant from this data. The choice of an
62 overly complex model would thus make the parameter estimation impossible. On the other hand, it can be
63 expected that while the parameters estimation of a very simple model would be much easier, the choice of an
64 overly simple model could limit the simulation accuracy due to its inherent uncertainty. Regarding the choice
65 of the set of equations for the simulation of the PV power production from amongst the different models
66 available in the literature, a compromise is thus required between minimizing the amount of information on
67 the PV plant needed by the model and maximizing the model accuracy.

68 To find the optimal model, the choice of the PV model considers different PV plant characteristics and
69 their respective effects on the power output. First, all processes occurring in a PV plant, whose consideration
70 with the chosen approach is unrealistic, were neglected (e.g. local shading, the effect of wind on the module
71 temperature, voltage-dependency of the inverter efficiency...). The characteristics of a PV plant to which
72 the output power is most sensitive were then identified. These are the two module orientation angles, the
73 set of parameters describing the optical losses of the module glazing, the electrical characteristics of the
74 power module and the power curve of the PV inverter. This information is important for the choice of the
75 set of models describing the different parts of a PV plant. Indeed, in order to decrease the modelling error,
76 accurate models should be preferred to describe the effects these key characteristics on the output power.

77 In contrast, simpler models can be chosen for other parameters whose effect on the power is lower. Based
78 on these considerations, a set of models to simulate the output power from meteorological data has been
79 selected from amongst those available in the literature. The resulting calculation steps are described in the
80 following paragraphs.

81 With the effect of local shading being neglected, the plane of array (POA) irradiation can be estimated
82 from the global irradiation and the sun position using a set of models commonly used for this purpose (Iqbal,
83 1983; Quaschnig, 1999). Here, the separation and transposition models proposed by Skartveit et al. (1998)
84 and Perez et al. (1993) are each respectively used for estimating the plane of array irradiation from the
85 global horizontal irradiation. The module azimuth and tilt angle as well as the ground albedo are the PV
86 plant information required for this first step. To limit the number of model parameters and considering its
87 limited effect on the output power, the ground-albedo is assumed to be constant and equal to 20%.

88 To estimate the POA irradiation effectively contributing to the photovoltaic effect (effective irradiation),
89 optical losses occurring within the module glazing have to be considered. The formulation of Martin and
90 Ruiz (2001) for calculating the angular losses has been chosen from the models existing in the literature
91 (Souka and Safwat, 1966; Standard et al., 1977; King et al., 1997) as it offers the best compromise between
92 simplicity and physicality. Indeed, Martin and Ruiz propose an analytical model based on theoretical and
93 experimental results that only requires two parameters (the angular loss coefficient and a fitting coefficient
94 for the diffuse and reflected irradiation) for the determination of the angular losses of the direct, diffuse
95 and reflected irradiances. As the output PV power is little sensitive to the fitting coefficient of the Martin
96 and Ruiz (2001) model for the diffuse and reflected irradiation, it is assumed constant and set to a value
97 representative for crystalline modules (0.07).

98 The influence of the variations of the solar spectrum on the power production of PV cells is neglected so
99 that the output of the PV power modules can be directly evaluated with the effective irradiation and the
100 module temperature.

101 The calculation of the module temperature can be nontrivial, as it is affected by local conditions (wind
102 cooling the module back-side, thermal inertia of the building, etc...). However, a detailed modelling of
103 the module temperature requires information on a PV plant that cannot be considered in the proposed
104 approach. As a result, the expression proposed by Ross (1976) has been chosen, where the difference
105 between the module and air temperature is assumed to be proportional to the POA irradiation.

106 Further models may be chosen for the remaining calculation steps that would result in a relatively large
107 set of additional parameters describing the respective influences of the PV module characteristics, DC-losses,
108 inverter efficiency, and so on, on the output power. A general consideration of the remaining simulation
109 steps however shows that a unique value of the produced power corresponds to each value of the effective
110 irradiation and module temperature. For the present application, individually modelling each component of
111 the plant is not necessary, since only their cumulative effect is needed for the power calculation. Accordingly,

112 a pragmatic simplification was made, using a look-up table (LUT) describing the combined behaviour of
113 the PV module, cable losses, inverter efficiency, etc... rather than simulating each effect individually
114 Additionally, with the assumption that the difference between module and air temperature is proportional
115 to the POA irradiation (Ross, 1976), it can be shown that the explicit simulation of the module temperature
116 can be avoided. Indeed, under this assumption, a single power value corresponds to any pair of effective
117 irradiation and air temperature. It was thus decided to use a look-up-table giving the output PV power for
118 all values of the effective irradiation and air temperature.

119 An advantage of the look-up-table is that parameters which are difficult to assess are implicitly considered
120 (effective capacity, soiling loss, mismatch losses, etc...). Furthermore, eventual modelling weaknesses are
121 avoided since it is not necessary to choose a mathematical model describing a relationship between the
122 input and output data. The use of an LUT may therefore not necessarily lead to a reduction of the model
123 accuracy. Finally, the use of an LUT instead of a set of additional parameters actually considerably simplified
124 the estimation of the model parameters from historical measurements (see following section).

125 In total, the chosen PV plant model uses three parameters (the module azimuth and tilt angles and
126 the angular loss coefficient) and an LUT describing the “total power curve” of the PV plant. A flow chart
127 illustrating the PV model is given in Figure 1. The input meteorological data are the global horizontal
128 irradiation and the air temperature (upper row) and the PV plant parameters are the module orientation
129 angles, the angular losses parameter and the LUT (left column).

130 One last issue remains to be addressed regarding the physical model. The power output of an increasing
131 number of PV plant is capped when the power exceeds a certain level (i.e. 70% of the peak capacity).
132 This limitation on the power is commonly referred to as inverter clipping. Though inverter clipping is not
133 explicitly discussed in this section, it is implicitly considered in the look-up table. Indeed, all irradiation
134 and temperature values leading to power values larger than the limit under normal conditions are associated
135 with the clipping limit. The effect of the power limitation is therefore contained in the look-up table and
136 no specific measure is required to consider the effect of inverter clipping.

137 3. Determination of the simulation parameters of a PV plant

138 With a PV model chosen, it remains to discover how the set of parameters best describing a PV plant
139 can be evaluated from power measurements. The basic idea is to identify the set of parameters with which
140 power simulated from meteorological data best matches with the measurements. Two issues need however
141 be clarified prior to the parameter search (section 3.3). Firstly, it is unclear what meteorological data are
142 the best suited for the determination of the configuration parameters (section 3.1). At the same time, given
143 the presence of a look-up-table in the model parameters and that measurements can be affected by issues
144 such as power line failures, it is unclear what cost function is suited to the present problem (section 3.2).

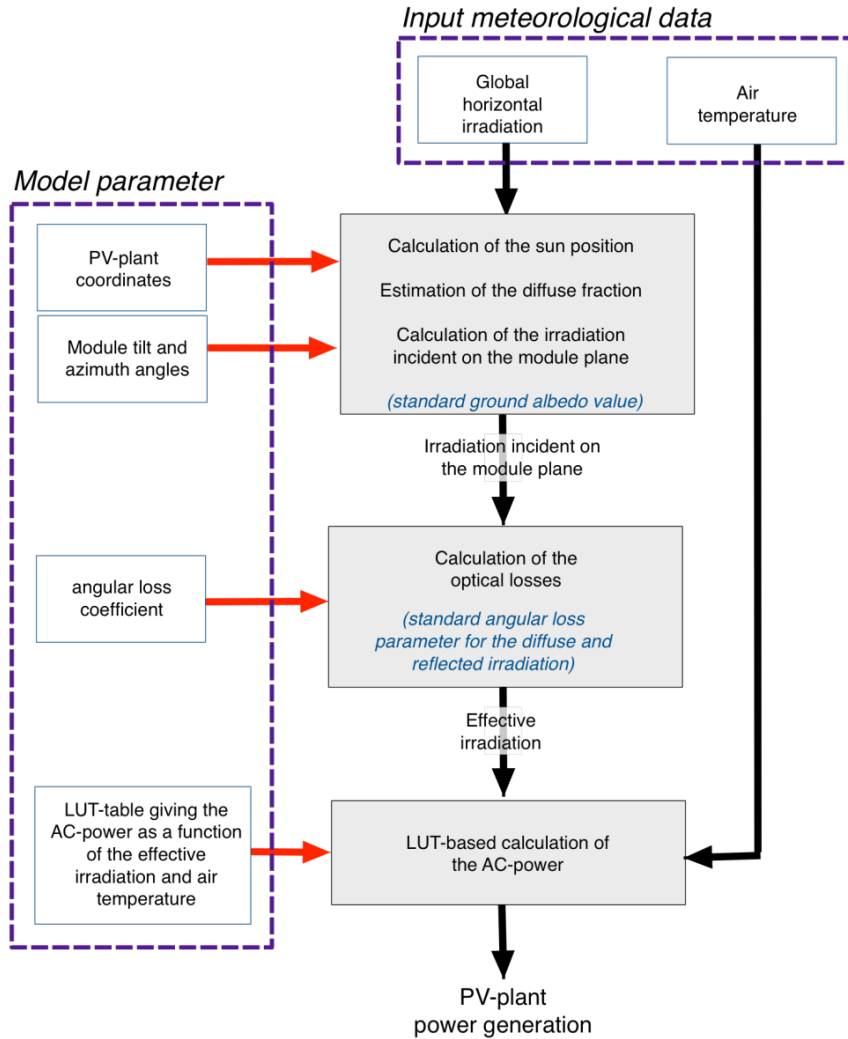


Figure 1: Flow chart of the simplified PV plant model

145 3.1. Choice of meteorological input data for the model parameter evaluation

146 Apart from its configuration (parameters of the PV model), the power production of a PV plant depends
 147 on the solar irradiation and the air temperature. The first step in the determination of the simulation
 148 parameters of a PV plant thus consists in collecting meteorological data for each point in time a measurement
 149 is available.

150 Should the present approach be needed to calculate PV power forecast, it may appear at first glance
 151 natural to use irradiation and temperature forecast to estimate the configuration parameters of the con-
 152 sidered plant. Deviations between forecasted and actual weather conditions when the power was measured
 153 may however result in noise that limits the performance of the parameter estimation. It is thus preferable
 154 to use the most accurate meteorological information available as an input for the parameter estimation.

155 Two situations can occur at this preliminary step. In the optimal situation, irradiation and temperature
156 are measured parallel to the AC power production. In this first situation, the meteorological information
157 needed for the power calculation is available directly from the set of measurements. A more common
158 situation is that only the power generation is measured and another source of meteorological data must
159 consequently be used. In this latter case, it is possible to extract for example irradiation from satellite-based
160 products and temperature from NWP analysis for the desired location and time period.

161 *3.2. Choice of the cost function*

162 Once meteorological data is available for each value of the power measurement, it remains to identify
163 with which set of parameters the PV power simulated from meteorological data best fits the measurements.
164 This is a common optimization problem that can be solved by choosing a cost function to quantify the
165 simulation error and by searching for its global minimum over the parameter space.

166 At first glance, it may seem natural to choose a common measure of the simulation error such as the
167 RMSE or MAE as the cost function. In practice, the implementation of this approach is difficult due to
168 the existence of a look-up table in the parameter set. Indeed, each value contained by the LUT needs to
169 be estimated by the optimization, such that the parameter space is too large for the optimization. Another
170 approach (or problem formulation) is thus necessary to solve the issue caused by the LUT.

171 The use of a look-up table in the simplified model has been motivated by the fact that, with the assumed
172 simplifications, a single value of the output PV power corresponds to any pair of air temperature and effective
173 irradiation values. This characteristic of the chosen PV model can also be exploited to evaluate the optimal
174 module orientation angles and optical loss coefficient (the LUT is not considered in a first time). Indeed,
175 these three parameters can be expected to have the following effects:

- 176 • If the module orientation angles and the optical loss coefficient are optimally chosen, little dispersion
177 should be observable amongst measurements corresponding to similar values of the simulated effective
178 irradiation and temperature (e.g. left-side plot in [Figure 2](#)).
- 179 • In contrast, a sub-optimal set of parameters should result in a higher dispersion among measurements
180 corresponding to similar values of the simulated effective irradiation and temperature (e.g. right-side
181 plot in [Figure 2](#)).

182 Based on the considerations above, it should be possible to search for the three parameters (module tilt
183 and azimuth angles and angular loss coefficient) by minimizing the dispersion of the measurements for any
184 values of the effective irradiation and temperature. The advantage of this approach is that the shape of the
185 power curve (quantified by the LUT) is not necessary for the optimization, which only focuses on maximizing
186 the density of points on this unknown power curve. As a result, the parameter space is reduced to the three
187 dimensions formed by the module tilt and azimuth angles and the angular loss coefficient. To implement

188 this idea, a cost function must still to be chosen that quantifies the dispersion of the measurements for any
 189 values of the effective irradiation and air temperature.

190 For a given set X_{param} of the three model parameters (module azimuth angle, module tilt angle and
 191 angular loss coefficient), the effective irradiation can be calculated from the global horizontal irradiation.
 192 Three time series are thus available as input data for the cost function: power measurements, air temperature
 193 and effective irradiation.

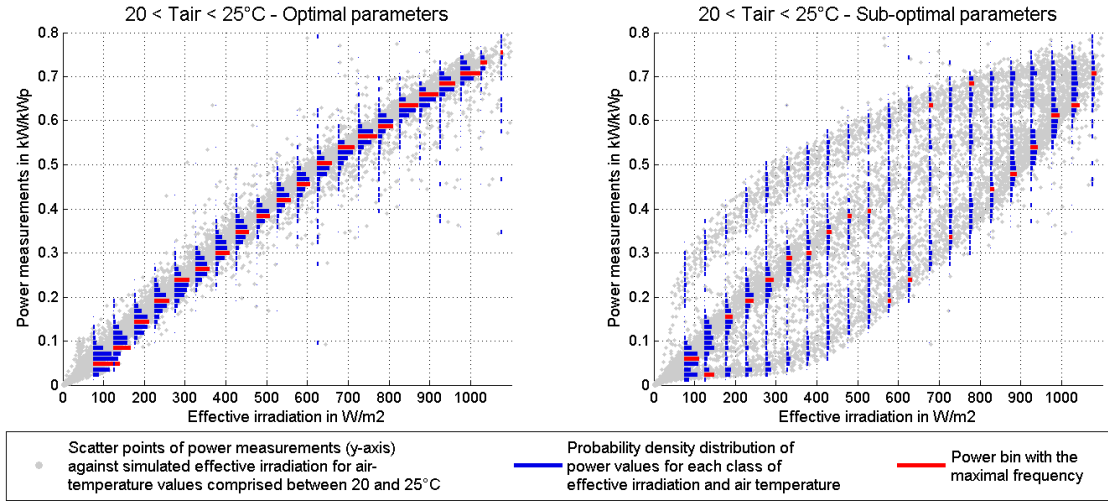


Figure 2: Illustration of the approach used for estimating the performances of a given set of parameters.

194 The dispersion of the data is first evaluated by calculating the joint probability distribution of the three
 195 considered variables. For this purpose the number of occurrences of the three considered quantities within
 196 different bins is counted. Bin widths of $0.01kW/kW_p$, $20W/m^2$ and $2^\circ C$ have been used for the power,
 197 irradiation and air temperature, respectively. This first step is illustrated in Figure 2 for air temperature
 198 values ranging between 20 and $25^\circ C$ and for a set of optimal and sub-optimal parameters (left and right
 199 picture respectively). Scatter points represent the adequacy between power measurements (ordinate) and
 200 simulated effective irradiation (abscissa). The number of values present in different power bins for each class
 201 of effective irradiation is represented by a horizontal bar. This operation is conducted for each class of air
 202 temperature. The meaning of the bar colours is discussed later.

203 The joint probability distribution concerns the distribution of the dataset in the entire space covered by
 204 the data. Since only the frequency of the occurrence of power values in the vicinity of the (unknown) power
 205 curve is needed, it remains to extract this information from the joint probability distribution.

206 When the set of parameters is optimal, it can reasonably be expected that the frequency of measurements
 207 will be higher for power bins corresponding to the power curve than for those elsewhere. In this case, the
 208 required information can thus be assessed for any value of the temperature and irradiation by selecting the

209 bin with the maximal frequency from amongst all bins of power measurement. These bins are marked in red
 210 in the example given on the left picture of [Figure 2](#). A final summation over all temperature and irradiation
 211 bins should give approximately the percentage of measurements lying in the vicinity of the unknown power
 212 curve (sum of frequency corresponding to all red bars in the left picture of [Figure 2](#)).

213 When the set of parameters is sub-optimal, the assessment described above becomes meaningless since it
 214 can no longer be expected that the power bin with the maximum frequency corresponds to the power curve.
 215 This situation is illustrated by the right picture in [Figure 2](#). However, in this case, the previous calculation
 216 should lead to a lower value than when optimal parameters are used. Indeed, based on the example given
 217 in [Figure 2](#), red bars are higher in the left (optimal parameter set) than in the right picture (sub-optimal
 218 parameter set). In that sense, this approach can still be used to evaluate the performances of a set of
 219 coefficients.

220 Finally, the cost function used for the estimation of the module azimuth angle, the module tilt angle and
 221 the angular loss coefficient is thus:

$$f^{cost}(X_{param}) = \sum_{j,k} \left[\max_i (p(PW_{Meas} = PW_i, G_{eff}(G_{hor}, X_{param}) = G_j, T_{air} = T_k)) \right] \quad (1)$$

222 Where:

- 223 • X_{param} is the set of considered parameters (module azimuth angle, module tilt angle and optical
 224 loss coefficient),
- 225 • $PW_{Meas}, G_{hor}, T_{air}$ are the power measurements, the global horizontal irradiation and air temper-
 226 ature data, respectively,
- 227 • $G_{eff}(G_{hor}, X_{param})$ is the effective irradiation calculated from G_{hor} with the parameter set X_{param} ,
- 228 • PW_i, G_j, T_k are the i^{th} , j^{th} and k^{th} bins of the power, irradiation and air temperature, respectively,
- 229 • $p(X = X_i, Y = Y_j, Z = Z_k)$ is the probability that X, Y and Z are equal to X_i, Y_j and Z_k (joint
 230 probability distribution), and,
- 231 • $f^{cost}(X_{param})$ is the cost function for the set of parameters X_{param} .

232 3.3. Determination of the configuration parameters

233 Using time series of power measurements and the corresponding irradiation and temperature data, the
 234 first three parameters can be evaluated by finding the set of parameters X_{param} that maximizes the cost
 235 function introduced in the previous section (1):

$$X_{Param}^{Opt} = \operatorname{argmax} (f^{cost}(X_{Param})) \quad (2)$$

236 This optimization is made in a three-dimensional space formed by the module tilt angle, the module
237 azimuth angle and the optical loss coefficient, so that the estimation of the first three parameters is relatively
238 fast.

239 Once the three parameters that maximises the cost function are found, the next step of the algorithm
240 consists in evaluating the look-up table that corresponds to the power curve of the PV plant. For this
241 purpose, the simulated effective irradiation, air temperature and power measurements are used and the
242 evaluation is made in two steps.

243 In the first step of the evaluation, for any value of the effective irradiation and air temperature, the
244 power curve value is evaluated as the most frequent value of the power measurement (bin with the largest
245 number of power measurements). These are represented by the red bars in [Figure 2](#). The most frequent
246 (or modal) value is preferred over e.g. the average value because it was judged to be more stable given the
247 problems potentially affecting the measurements (line outage, measurement errors, etc. . .).

248 At this stage, only values of the effective irradiation and air temperature covered by the measurement
249 dataset can be evaluated in the look-up-table. This would not be a problem if the measurement dataset
250 were sufficiently large such that all possible values of air temperature and effective irradiation were covered.
251 However, it cannot be excluded that a simulation could require a value from the look-up table that could
252 not be assessed with the available measurements. An estimation of the values undefined in the look-up-table
253 was thus necessary, which is the second step of the evaluation.

254 For the purpose of the estimation of the undefined LUT values, a linear dependency between the output
255 power and the air temperature for each value of the effective irradiation is assumed. With this assumption, at
256 each value of the effective irradiation, the two coefficients describing the linear dependency between output
257 AC-power and air temperature are estimated with the available data and the undetermined values of the
258 look-up table are filled by extrapolating the data with this linear relationship.

259 4. Sample applications

260 4.1. Test PV plants

261 Two PV plants have been chosen to illustrate the performances of the parameter estimation algorithm
262 presented in this paper. These plants have been selected from amongst numerous plants for which the
263 algorithm has been implemented, with the intention of demonstrating not only the performances obtained
264 but also of showing the limitation of the proposed approach. Power measurements used in the two chosen
265 examples are thus affected by local shading and measurement errors. Measurement errors have been inten-
266 tionally left in the dataset for assessing how the proposed approach copes with such issues. This is discussed
267 later in the validation of the results.

268 The measurements of two plants provided by the Technical University of Bern have been chosen to
 269 illustrate the operation and evaluate the performance of the proposed algorithm. A short description of the
 270 two PV plants used is given in Table 4.2.

	Stade de Suisse Wankdorf (DA1)	EBL Liestal
Latitude	46°57'51"	47°29'16"
Longitude	7°27'55"	7°46'59"
Year of installation	2005	1992
Azimuth and tilt angles ¹	-63° E / 20.5°	0° S / 30°
Peak power	127.575kW _p	18.510 kW _p
Reference of module	Kyocera KC-167GH-2	Kyocera LA361H51
Number of modules	729	363
Reference of inverter	Sputnik SolarMax125	Sputnik SolarMax20
Period used for the parameter estimation	01.01.2008 – 31.12.2008	01.01.2009 – 31.12.2009

Table 1: Description of the characteristics of the EBL Liestal PV plant.

271 For these two plants, one year of five-minute measurements of the output AC-power, global horizontal
 272 irradiation, POA irradiation, air temperature and module temperature are available.

273 For both plants the algorithm has first been run with local meteorological measurements and then
 274 using remote-data. Remote data include irradiation calculated from satellite images with the helioclim-3v4
 275 method (Espinar et al., 2012) and air temperature taken from Cosmo-DE analysis (Schulz and Schättler,
 276 2014). Where remote data have been used fifteen-minute average power measurements have been evaluated
 277 to match the time resolution of the satellite data. The original time resolution of five minutes has been used
 278 when the algorithm is run with local meteorological measurements.

279 4.2. Validation of the estimated parameters

280 For the sake of brevity, the optimization conducted for the estimation of the parameters is not detailed
 281 in this paper. Alternatively, reports generated by the algorithm are given in the appendix for each algorithm
 282 run conducted. These reports provide an overview of all end- and intermediary results, which are important
 283 for assessing the quality of the parameter estimation. Only the final results of the algorithm are discussed
 284 in this section.

285 Module orientations and optical loss coefficients found with the algorithm are given in Table 4.2 and
 286 scatter plots of the normalized measured power (y-axis) as a function of the effective irradiation (abscissa)
 287 are displayed in ??.

Meteorological data used for the parameter estimation	Estimated parameters	Stade de Suisse Wankdorf (DA1)	EBL Liestal
Local irradiation and temperature measurements	Azimuth angle	-68°E	-3°E
	Tilt angle	22°	30°
	Optical loss coefficient	0.14	0.25
Satellite-derived irradiation and Cosmo-DE analysis temperature	Azimuth angle	-68°E	-1°E
	Tilt angle	22°	30°
	Optical loss coefficient	0.06	0.085

Table 2: Illustration of the approach used for estimating the performances of a given set of parameters.

Table 3: Results of the parameter estimation.

288 The module orientation angles estimated with the algorithm can be directly compared with the values
289 available from the plant description. A validation of the angular loss coefficient and power curve look-
290 up table is by contrast not possible, as the actual values of these parameters are not available from the
291 plant information. An indirect validation of these parameters is therefore realized by verifying that the
292 estimated power curve matches the dependencies between power measurements, effective irradiation and air
293 temperature.

294 Validation of the estimated module orientation angles

295 The module orientation angles evaluated by the algorithm and those provided by the plant operator can
296 be found in and respectively.

297 There is a good agreement between module orientation angles found with local meteorological measure-
298 ments and remote data. For the Liestal plant the module orientation found with the local and remote data
299 are (-3°E; 30°) and (-1°E; 30°) respectively, while the same module orientation has been found with the two
300 datasets for the Wankdorf PV plant (-68°E; 22°).

301 The module tilt angle found at Liestal corresponds exactly to that provided by the plant operator (30°).
302 In contrast, estimated azimuth angles correspond to a slightly eastward orientation (-3°E and -1°E) while
303 a southern orientation is indicated in the plant description. An aerial view of the plant taken from Google
304 Earth (left picture in Figure 3) reveals that the plant is indeed slightly oriented to the east, such that the
305 results of the algorithm are plausible.

306 In the left picture of Figure 3, it can also be observed that a part of the PV plant is shaded in the
307 morning. The production deficit resulting from the shading may explain the higher dispersion of the scatter
308 points in the two right plots from Figure 5 for an effective irradiation between 0 and 600W/m².

309 A larger discrepancy is found between module orientations given by the plant operator (-63°E; 20.5°)
310 and those found by the algorithm (-68°E; 22°) in the second example (Wankdorf Stade de Suisse). The
311 difference in tilt angle is relatively small (overestimation of +1.5°) but the larger azimuth angle difference
312 of 5° is not negligible. A control of the module orientation with Google Earth (right picture in Figure 3)

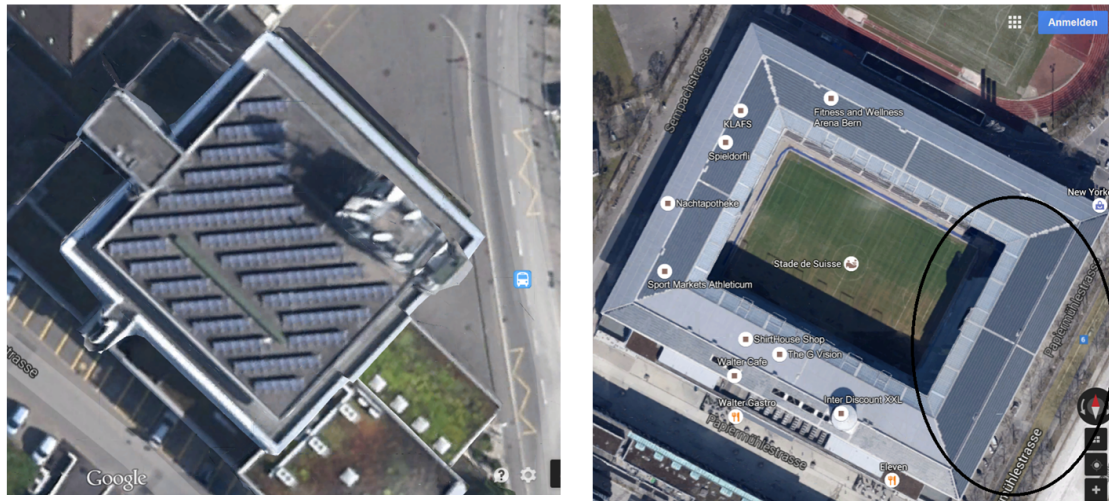


Figure 3: Aerial view of the Liestal (left picture) and Wankdorf Stade de Suisse PV plants (right picture) Source: Google earth

313 confirmed that the azimuth angle provided by the plant operator (-63°E) is correct. The module orientation
 314 estimated by the algorithm therefore seems to deviate from its actual value for this plant.

315 Numerous intermediate measurements available from the Wankdorf PV plant (POA irradiation, air and
 316 module temperature, DC and AC power) allowed for the validation of the different steps of the PV power
 317 calculation in order to understand the reason for this difference. An analysis of these intermediate results
 318 revealed that this difference in the azimuth angle results from the assumption made for modelling the
 319 module temperature. Indeed, the Ross model was chosen, in which the difference between the module and
 320 air temperature is assumed to be proportional to the POA irradiation. This implies that a single module
 321 temperature corresponds to each value pair (POA irradiation and air temperature). The analysis of the
 322 intermediary measurements showed that the characteristics of the module temperature do not fully satisfy
 323 this simplifying assumption.

324 To highlight the behaviour of the module temperature responsible for the deviation of the estimated
 325 azimuth angle from its actual value, differences between measured module and air temperature are displayed
 326 as a function of the measured POA irradiation in Figure 4. Since a dependence of the scatter points with
 327 the time of the day was identified, scatter points have been coloured according to the solar azimuth angle.

328 It can be observed in Figure 4 that for a given POA irradiation the difference between the module and air
 329 temperature is lower in the morning than in the afternoon. For example, for a POA irradiation of $400\text{W}/\text{m}^2$,
 330 a temperature difference of 10°C is observed at a solar azimuth of 120° , while it increases to 20°C as the solar
 331 azimuth is 240° . Under the same external conditions (air temperature and POA irradiation), a difference
 332 depending on the solar azimuth reaching up to 10°C can thus be observed, which is inconsistent with the
 333 simplifying assumption made.

334 The observed dependency of the module temperature on the solar azimuth (or the time of the day) can be

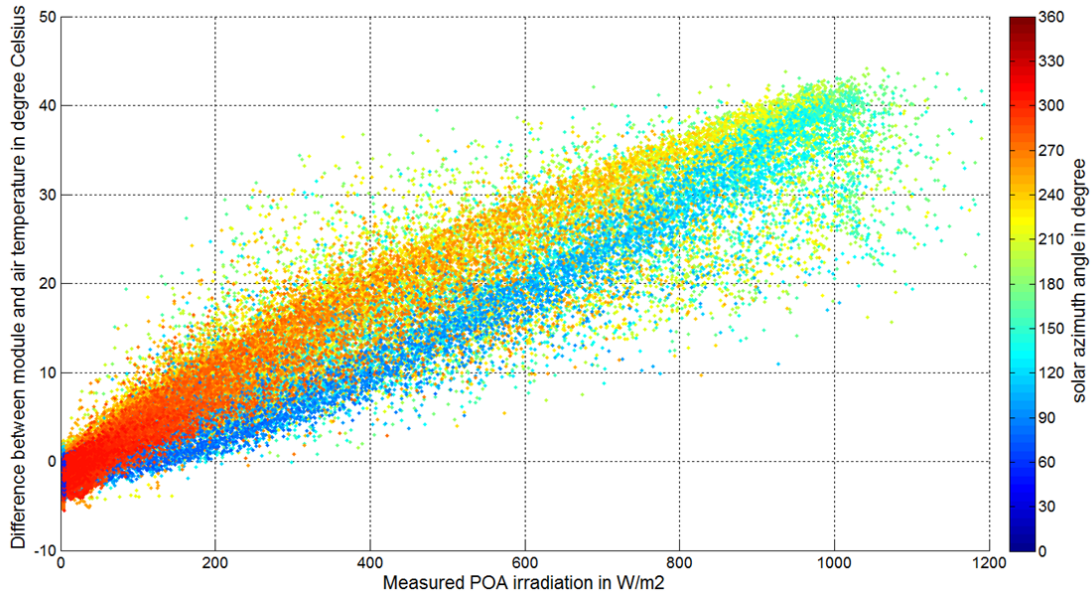


Figure 4: Dependence of the difference between the module and air temperature (ordinate) on the POA irradiation (abscissa) and the solar azimuth angle (colour of the scatter points) for the Wankdorf PV plant.

335 easily explained by the fact that the PV modules are directly integrated on the roof of the Wankdorf stadium.
 336 The air behind the module is heated by the incoming irradiation in the course of the day, which heats the
 337 backside of the PV module so that the module temperature exhibits a dynamic behaviour influenced by the
 338 thermal inertia of the building. As the consideration of the thermal inertia of the module was not foreseen
 339 in the chosen model, the parameter estimation algorithm has balanced the resulting modelling error by
 340 overestimating the module azimuth angle.

341 As previously mentioned, an explicit consideration of effects such as those illustrated in Figure 4 have
 342 been intentionally omitted in the chosen PV model (they would have required information of excessive detail
 343 on a PV plant). It is thus clear that a modelling error may occur for plants like Wankdorf where the validity
 344 of the simplifying assumption is limited. Given that the proposed algorithm estimates model parameters
 345 by maximizing the probability that a simulation matches the measurements, it is not surprising that a set
 346 of parameters different from the actual ones is found at Wankdorf. In a way, it can be considered that the
 347 difference between the estimated and actual parameters compensates for the weaknesses of the simplified
 348 PV model for this plant.

349 **Validation of the angular loss coefficients and power curve LUT**

350 As already mentioned, a direct validation of the angular loss coefficient and power curve LUT is not
 351 possible, as their actual values are not available from the description of the PV plant. Therefore, an indirect
 352 validation has been conducted, where it was verified that these parameters describe well the dependence
 353 between the effective irradiation, air temperature and power measurements.

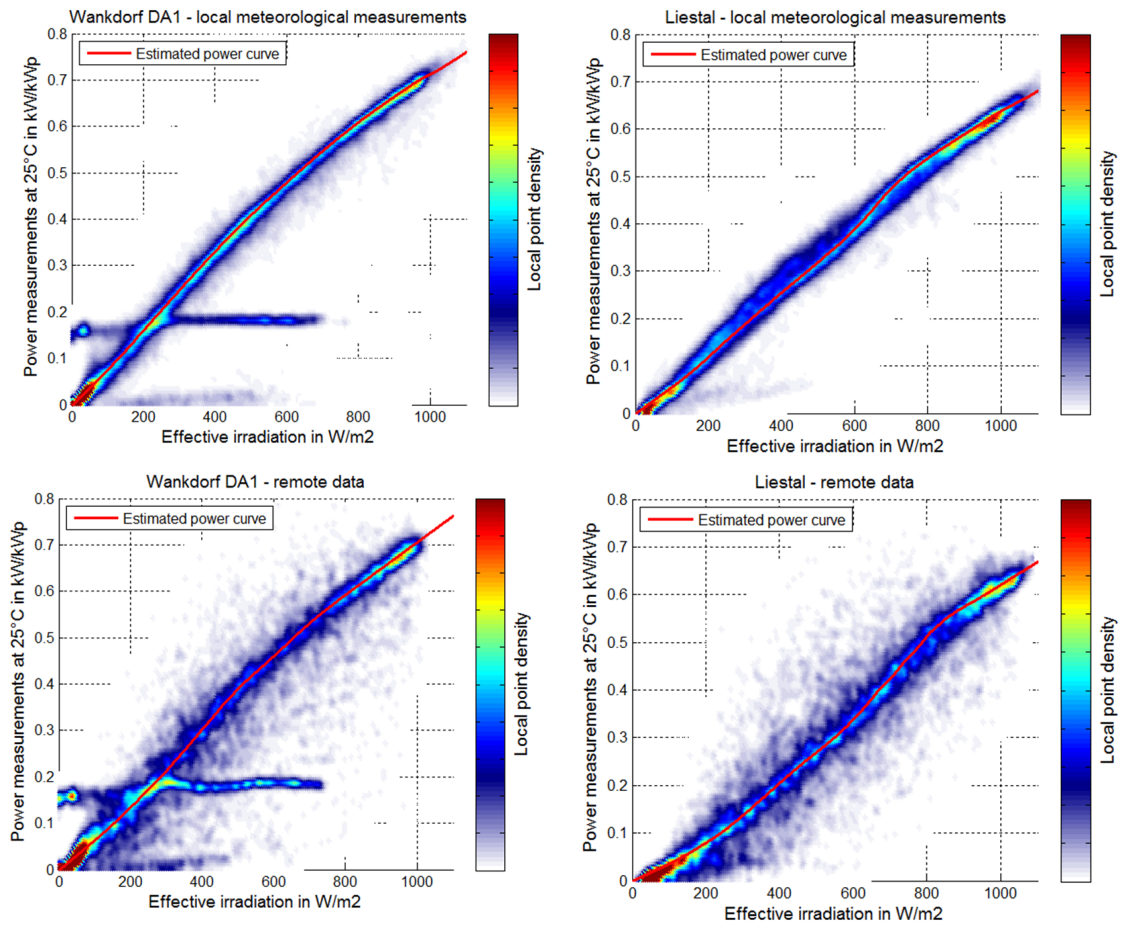


Figure 5: Scatter plots of the normalized measured power (ordinate) as a function of the effective irradiation (abscissa) and the estimated power curve (red line) – the colour of the scatter points represent the local point density.

354 In ??, scatter plots of the normalized measured power as a function of the effective irradiation can be
 355 found for the four algorithm runs. Power measurements were corrected for their dependency on the air
 356 temperature to facilitate the visualisation of the data. For this purpose, the linear dependency assessed
 357 during the construction of the look-up table (see previous section) has been used to evaluate AC-power
 358 values corresponding to an air temperature of 25°C. The colour of the points represents the local density of
 359 the scatter points. A light blue to blue point occurs rarely, while a red point is very frequent. The power
 360 curves corresponding to an air temperature of 25°C, evaluated by the parameter estimation algorithm, are
 361 displayed in each scatter plot by a red curve.

362 The scatter plot corresponding to the estimation of the model parameters of the Wankdorf plant using
 363 local meteorological measurements is displayed in the upper left picture in Figure 5. A line of scatter points
 364 with a high density (light blue to red dots) starting from the origin ($0W/m^2; 0kW/kW_p$) and ending at
 365 ($1000W/m^2; 0.7kW/kW_p$) can be observed in this figure, which corresponds to the power curve of the PV

366 plant. A horizontal line of scatter points with a high density can also be observed in this scatter plot. These
367 points result from a time period where values delivered by the data logger were constant (intentionally not
368 excluded from the dataset). It is interesting to note that these points did not seem to affect the algorithm,
369 which was expected, given the chosen cost function. The red line represents power curve values obtained
370 from the algorithm. The red line matches very well to the line of scatter points of high density. In this first
371 example, the module orientation and optical loss coefficient seem to be correctly estimated, as the scatter
372 plot contains a continuous line with a high density of points. The LUT evaluated by the algorithm seems also
373 very plausible because the estimated power curve matches well for regions of high scatter point density. In
374 this first example, the results of the algorithm are very plausible and the algorithm performance appears to
375 be insensitive to measurement errors. The same conclusion as that previously described can be drawn from
376 the observation of the scatter plot corresponding to the estimation of the parameters of the Wankdorf plant
377 using remote data (lower left picture in ??). More noise than in the previous plot can however be observed
378 here, which results from the uncertainty of the satellite-derived irradiation and the Cosmo-DE temperature.
379 The power curve obtained with remote data is very similar to that resulting from local meteorological
380 measurements. Lower values can however still be observed for values of the effective irradiation ranging
381 from 0 to $400W/m^2$. This difference may be explained by the difference in the angular loss coefficient
382 between the two runs, or by a bias in the satellite-derived irradiation. Despite these minor differences, it is
383 interesting to note that similar results are obtained with the algorithm when local measurements or remote
384 meteorological data are used.

385 The dispersion of scatter points corresponding to the parameter estimation of the Liestal PV plants
386 from local meteorological measurements (upper right picture in [Figure 5](#)) is larger than that observed at
387 Wankdorf (upper left picture in [Figure 5](#)). A visual inspection of the intermediate measurements available
388 showed that a module shading occurring in the morning at low solar elevation (already observed in [Figure 3](#))
389 is responsible for this spread. The red line matches well with scatter points of high density. However, it
390 is very likely that these points are affected by the shading and that the estimated power curve is lower
391 than the actual one. The same effects can be observed in the scatter plot corresponding to the parameter
392 estimation of the Liestal PV plants from remote data (lower right picture). In these last two examples, it is
393 interesting to note that correct module orientation angles were found despite the effect of the local shading
394 on the measurements.

395 5. Discussion and Conclusion

396 An algorithm has been developed that derives the parameters of a physical model from historical PV
397 power measurements. For this purpose, a simple PV model fulfilling the requirements of the intended
398 application has been chosen (??) and a parameter-estimation method dealing with usual issues occurring in

399 a PV plant (e.g. line outage, measurement errors) has been proposed in [section 3](#).

400 The operation and performance of the algorithm have been illustrated for two PV plants in [section 4](#).
401 Outputs of the algorithm were found to be plausible and in good agreement with the information available
402 on the PV plants. It was found that the parameters estimated with the algorithm may deviate from their
403 actual values when, due to modelling error, they result in better simulation results. In this sense, the output
404 of the algorithm should be seen as a set of parameters that lead to the best simulation and not necessarily
405 as the actual characteristics of the PV plant. Nevertheless, a physical interpretation of the algorithm output
406 is possible albeit with some precaution.

407 With the chosen cost function, the algorithm was shown to be little sensitive to outliers resulting from
408 measurement errors or power line outages, which constitutes an advantage in comparison to statistical
409 methods. The performance of the proposed method were found to be limited when PV module are shaded.
410 In that case, for the considered examples, the module orientation was correctly assessed but the power curve
411 was underestimated for power values affected by the shading. An explicit consideration of this issue could
412 improve the proposed approach in the future.

413 The algorithm has been tested with several hundred PV plants. These have shown that at least six
414 months of power measurements are necessary for an accurate estimation of the module tilt angle. When
415 less than six month measurement is available and should the module orientation angles be available from
416 plant information, it is possible to only assess the optical loss coefficient and the power curve of the plant by
417 setting orientation angles to their known value. With regards to this, the proposed method is much more
418 flexible than traditional statistical or physical approaches. It has also been shown that its performance is
419 limited in some situations. For example, it often occurs that a power production time series corresponds to
420 the aggregated production of modules with different orientations. The algorithm performs poorly in such
421 cases, since it is based on the assumption that only a single orientation exists for a PV plant. A simulation
422 error was also observed to result from the assumption that soiling losses are constant with time.

423 The parameter assessment algorithm described in this paper is German patent pending ([Saint-Drenan](#)
424 [and Bofinger, 2012](#)).

425 **Acknowledgements**

426 The authors thank the Technical University of Bern for their valuable measurements, which allowed
427 validating and understanding the limitation of the method presented in this paper. The authors are indebted
428 to Lucien Wald and Philippe Blanc for their help in understanding the Helioclim data. We would also like
429 to thank the Transvalor team, which is in care of the SoDa Service that makes the access to the Helioclim
430 databases efficient and user-friendly.

431 **References**

- 432 de Rocha Vaz, A. G. C., 2014. Photovoltaic forecasting with artificial neural network. Ph.D. thesis, University of Lisbon.
- 433 Dolara, A., Grimaccia, F., Leva, S., Mussetta, M., Ogliari, E., 2015. A physical hybrid artificial neural network for short term
434 forecasting of PV plant power output. *Energies* 8 (2), 1138–1153.
- 435 Drews, A., Lorenz, E., Betcke, J., Keizer, A., van Sark, W., Beyer, H. G., Heydenreich, W., Wiemken, E., Stettler, S.,
436 Toggweiler, P., Bofinger, S., Schneider, M., Heilscher, G., Heinemann, D., 06 2006. Remote performance check and automated
437 failure identification for grid-connected pv systems – results and experiences from the test phase within the pvsat-2 project.
- 438 Espinar, B., Aznarte, J. L., Girard, R., Moussa, a. M., Kariniotakis, G., 2010. Photovoltaic Forecasting: A state of the art. 5th
439 European PV-Hybrid and Mini-Gird Conference 33, 250–255.
440 URL <http://hal.inria.fr/docs/00/77/14/65/PDF/Espinar-Tarragona2010.pdf>
- 441 Espinar, B., Blanc, P., Wald, L., Gschwind, B., Ménard, L., Wey, E., Thomas, C., Saboret, L., 2012. HelioClim-3: a near-real
442 time and long-term surface solar irradiance database. In: COST WIRE workshop on "Remote Sensing Measurements for
443 Renewable Energy". p. 4 pp.
- 444 Iqbal, M., 1983. An Introduction to Solar Radiation. Academic Press.
445 URL <https://books.google.fr/books?id=BjCqswEACAAJ>
- 446 Kidwelly, P. (Ed.), 7 2006. PVSAT-2: Results of Field Test of the Satellite-Based PV System Performance Check. Vol. 4 of 5.
447 The organization, The name of the publisher, The address of the publisher, an optional note.
- 448 King, D. L., Kratochvil, J. A., Boyson, W. E., 1997. Temperature coefficients for PV modules and arrays: Measurement
449 methods, difficulties, and results. In: Conference Record of the IEEE Photovoltaic Specialists Conference. pp. 1183–1186.
- 450 Martin, N., Ruiz, J. M., 2001. Calculation of the PV modules angular losses under field conditions by means of an analytical
451 model. *Solar Energy Materials and Solar Cells* 70 (1), 25–38.
- 452 Perez, R., Seals, R., Michalsky, J., 1993. All-weather model for sky luminance distribution-Preliminary configuration and
453 validation. *Solar Energy* 50 (3), 235–245.
- 454 Quaschnig, V., 1999. Regenerative Energiesysteme, Technologie, Berechnung, Simulation, 2nd Edition. Hanser, von Volker
455 Quaschnig.
- 456 Ross, R. G., 1976. Interface Design Considerations For Terrestrial Solar Cell Modules. In: Proceedings of the 12th IEEE
457 Photovoltaic Specialists Conference. pp. 801–806.
458 URL <https://www2.jpl.nasa.gov/adv{ }tech/photovol/ppr{ }75-80/InterfaceDesConsid{ }PVSC76.pdf>
- 459 Saint-Drenan, Y.-M., Bofinger, S., Aug. 2012. Verfahren zur bestimmung von parametern einer photovoltaikanlage. DE Patent
460 DE102012214329A1.
- 461 Schulz, J., Schättler, U., 2014. Kurze Beschreibung des Lokal-Modells Europa COSMO-EU (LME) und seiner Datenbanken
462 auf dem Datenserver des DWD. DWD.
463 URL <https://books.google.fr/books?id=ku8JvwEACAAJ>
- 464 Skartveit, A., Olseth, J. A., Tuft, M. E., 1998. An hourly diffuse fraction model with correction for variability and surface
465 albedo. *Solar Energy* 63 (3), 173–183.
- 466 Souka, A. F., Safwat, H. H., 1966. Determination of the optimum orientations for the double-exposure, flat-plate collector and
467 its reflectors. *Solar Energy* 10 (4), 170–174.
- 468 Standard, A., et al., 1977. Methods of testing to determine the thermal performance of solar collectors. *American Society of
469 Heating*, 93–77.

470 **Panel (1):**

471 *The location of the PV plant is displayed on a map by a square whose colour corresponds to the maximum*
472 *value of the cost function evaluated by the algorithm at this location. The abscissa is the longitude and the*
473 *ordinate the latitude.*

474 *If the exact location of the PV plant is known, this map is trivial. Should the exact location of the plant*
475 *not be known but rather for example only the postal code, an estimation of the coordinates of the PV plant is*
476 *represented in this map. This is achieved by selecting all points where meteorological information is available*
477 *in a given area (for example all pixels of the satellite) and assessing the pixel with the highest value of the*
478 *cost function, which should serve as an approximation of the location of the PV plant.*

479 **Panels (2),(3):**

480 *An overview of the search of the maximum value of the cost function in the space formed by the three*
481 *unknown parameters is given in these two plots. With the cost function having been assessed for all values*
482 *in the three-dimensional space formed by the unknown parameters, the result of the optimization is a four-*
483 *dimensional array that requires simplification for a visualisation of the results.*

484 *In panel (2), the maximum value of the cost function obtained for each value of the module orientation*
485 *is displayed in colour as a function of the azimuth angle (abscissa) and tilt angle (ordinate). A blue square*
486 *represents a small value of the cost function and a red pixel a high value of the cost function (no colour scale*
487 *is given). The module orientation corresponding to the maximum value of the cost function is displayed by a*
488 *white cross and the module orientation provided by the meta-information is represented by a white diamond.*

489 *In panel (3) the maximum value of the cost function obtained for each value of the angular loss coefficient*
490 *(ordinate) is represented as a function of the angular loss coefficient (abscissa). The red cross represents*
491 *the optimal angular loss coefficient.*

492 **Panels (4):**

493 *In this table, the available meta-information on the PV plant and the results of the parameter estimation*
494 *are summarized. Common statistical measures of the simulation error obtained with the estimated parameters*
495 *and the used meteorological data are also indicated.*

496 **Panels (5),(6):**

497 *In panel (5), a scatter plot of the power measurements corrected for the temperature effect at 25°C*
498 *(ordinate) as a function of the effective irradiation (abscissa) is displayed. The colour of the scatter points*
499 *represents the local scatter point density. A blue point corresponds to a point with a low local density and a*
500 *red point to a high local density. The power curve estimated at 25°C is superimposed using a black dashed*
501 *line.*

502 *In panel (6), the effect of the air temperature (x-axis) on the PV power (ordinate) is illustrated for four*
503 *values of the effective irradiation. The different values of the effective irradiation are recognizable by the*
504 *colour of the scatter points (very light blue, light blue, blue and green points), which correspond to effective*

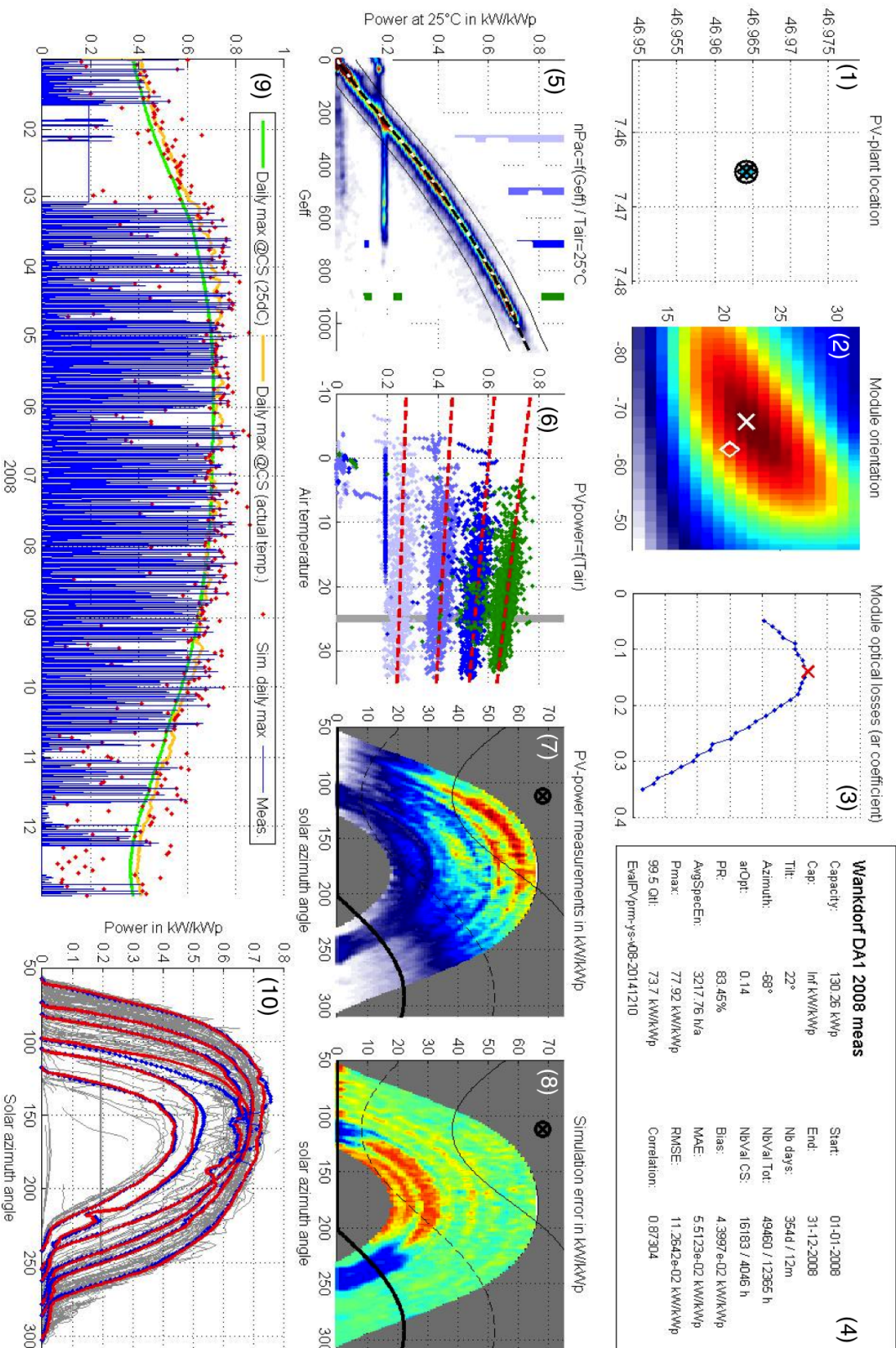


Figure 6: Report generated for the estimation of the parameters of the PV plant Wankdorf DAI using local meteorological measurements.

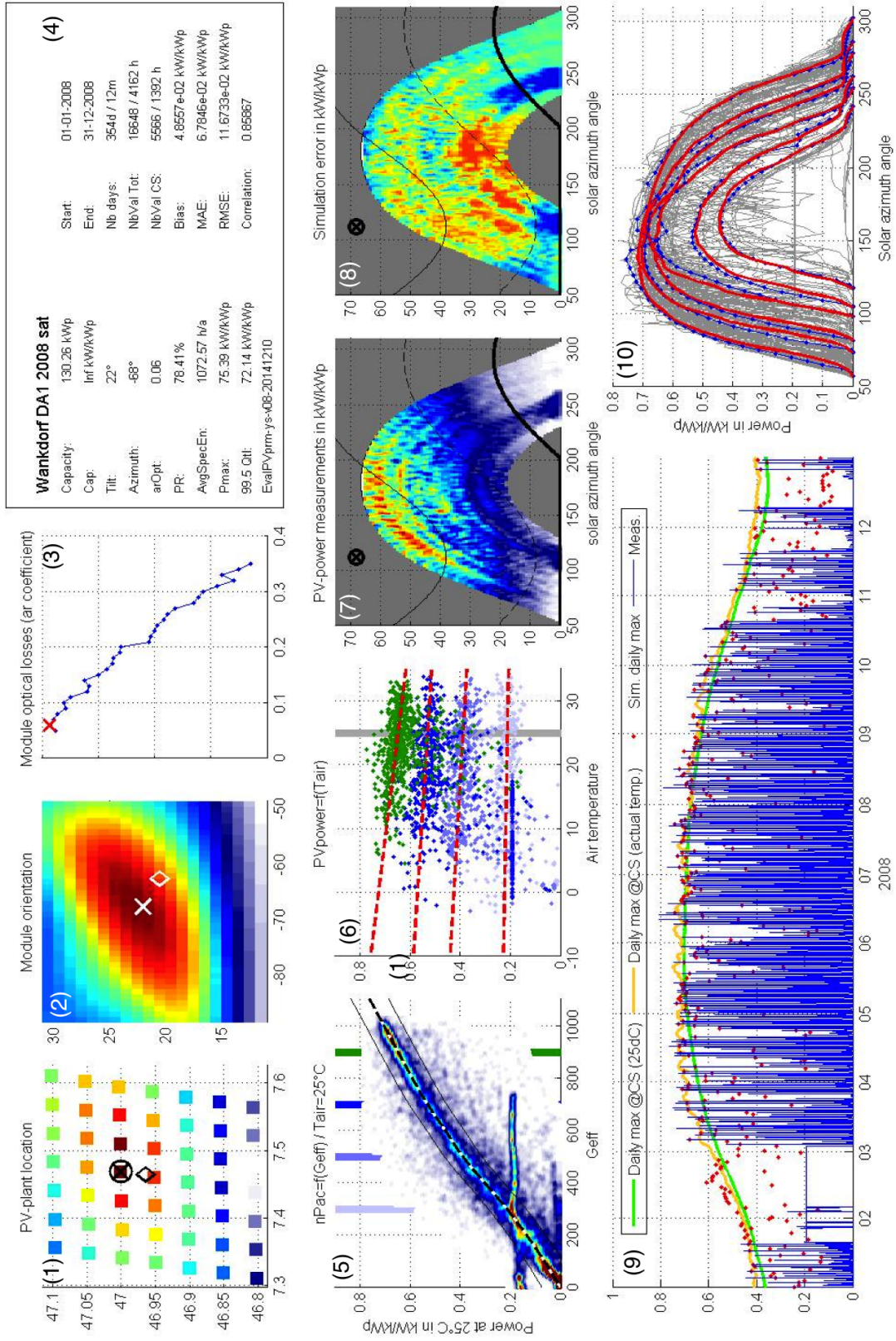


Figure .7: Report generated for the estimation of the parameters of the PV plant Wankdorf DA1 using satellite derived irradiation and analysis temperature.

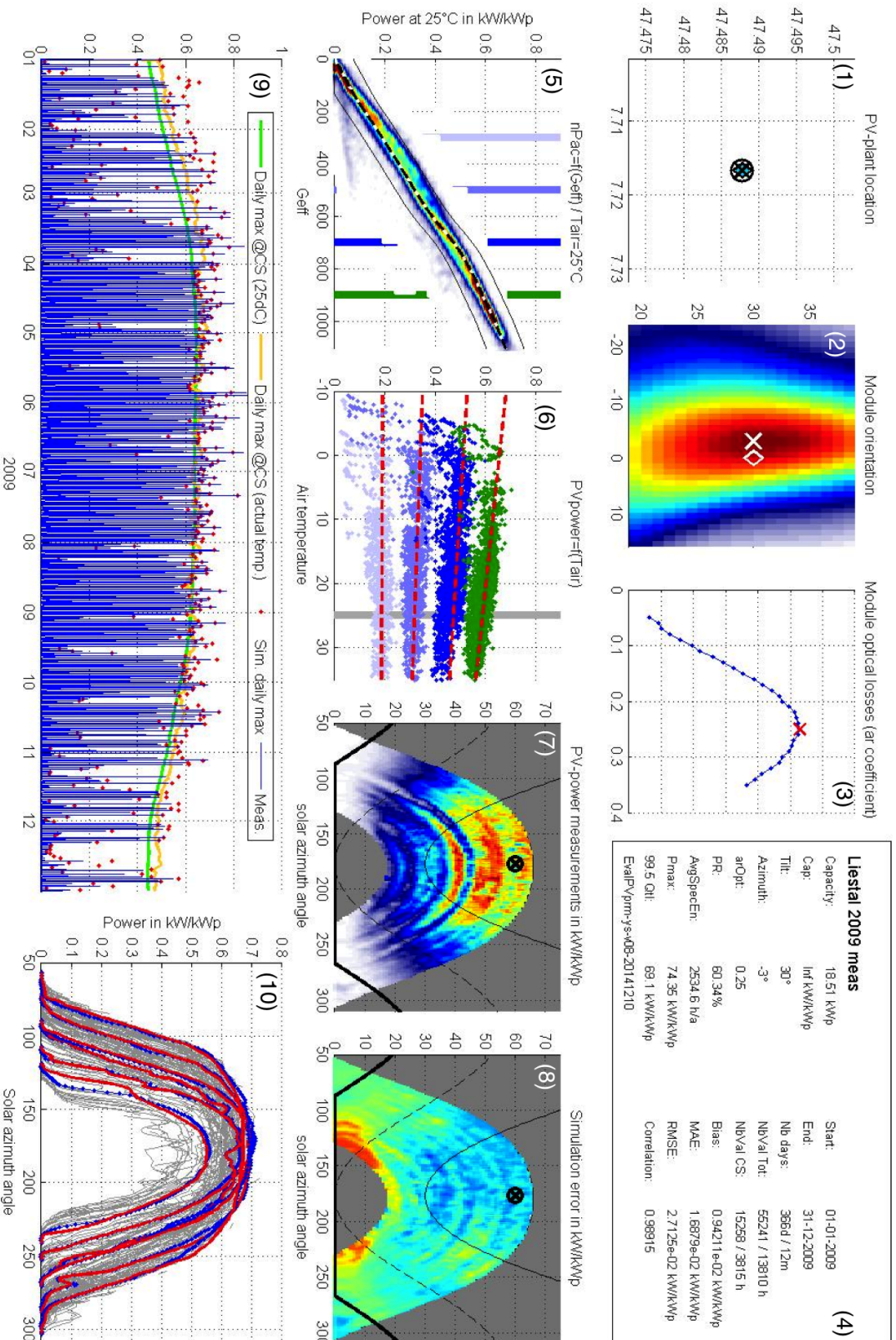


Figure 8: Report generated for the estimation of the parameters of the Liestal PV plant using satellite derived irradiation and analysis temperature.

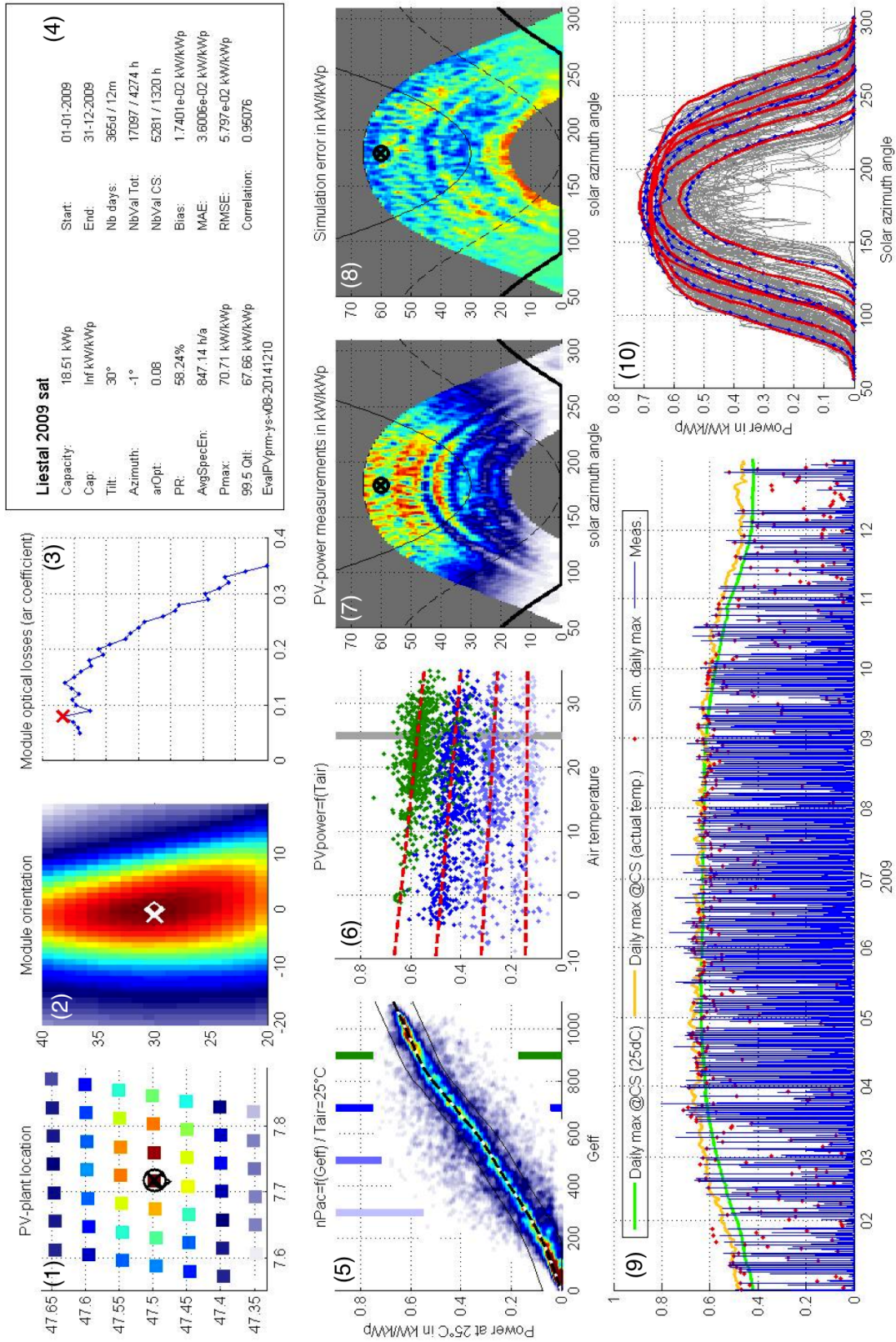


Figure 9: Report generated for the estimation of the parameters of the Liestal PV plant using satellite derived irradiation and analysis temperature.

505 irradiation values of 300, 500, 700 and 900 W/m², respectively. The red dashed lines are the values of the
506 LUT corresponding to the different effective irradiations.

507 **Panels (7):**

508 The measured power values (colour of the scatter points) are displayed as a function of the solar azimuth
509 (abscissa) and elevation angles (ordinate). White-to-blue points correspond to small power values (0 to 0.15
510 kW/kWp), while red points represent large power values (0.6 to 0.8 kW/kWp). Isolines of the incidence
511 angles resulting from the estimated module orientation are shown (90, 60, 30 and 0°). Under clear-sky
512 conditions, with the maximum power being reached at small incidence angles, a correspondence should be
513 observable between the scatter points and the isolines of the incidence angles. Thus, the comparison of the
514 two allows for verification of the estimated module orientation.

515 **Panels (8):**

516 The differences between the measurements and the power calculated with the estimated parameters (colour
517 of the scatter points) are displayed as a function of the solar azimuth (abscissa) and elevation angles (or-
518 dinate). A light green point corresponds to a simulation error close to zero while blue points (red points)
519 represent a simulated power 0.025 kW/kWp smaller (larger) than the measured power.

520 As in the previous plot, sun positions corresponding to incidence angles of 90, 60, 30 and 0° are displayed
521 by three black lines and a black circle, respectively. This representation can be useful for identifying local
522 shading effects on the power measurements.

523 **Panels (9):**

524 Time series of the simulation and measurements are compared for the entire training period. The mea-
525 surements are shown by the blue line. To improve the readability of this graphic all simulated values were not
526 displayed, but instead only the daily maximum of the simulated power. Additionally, the maximum daily sim-
527 ulated value that would have been reached under a clear-sky situation is represented by the yellow line. These
528 two values of the simulation allow for the quick verification of the yearly shape of the measurements being
529 well described by the simulation. These various outputs allow for verification that the seasonal variation of
530 the PV power is described well by the estimated parameters.

531 **Panels (10):**

532 With the focus of panel (9) being on the yearly behaviour of the power data, the daily behaviour is
533 represented in panel (10). For a better visibility, only clear-sky days are displayed here. Power measurements
534 are displayed as a function of the solar azimuth instead of as a function of time, in order to avoid the effect
535 of the yearly variation of the solar noon.

536 The power measurements are displayed for all selected clear-sky days by a light grey line. To avoid clutter,
537 simulated power values are only displayed for 5 days chosen arbitrarily from amongst the set of clear-sky
538 days. For these example days the measurements are displayed by a bold black line and the simulation by a
539 red line.